Open Access Library Journal
2025, Volume 12, e13916
ISSN Online: 2333-9721
ISSN Print: 2333-9705

Development of Electromechanical System for Antenna Positioning

Asif A. Mulla[1], Pramod N. Vasambekar[2]

[1]Department of Electronics, Yashwantrao Chavan College of Science, Karad, India
[2]Department of Electronics, Shivaji University, Kohlapur, India
Email: mulla.1984@gmail.com, pnv_eln@unishivaji.ac.in

How to cite this paper: Mulla, A.A. and Vasambekar, P.N. (2025) Development of Electromechanical System for Antenna Positioning. *Open Access Library Journal*, **12**: e13916.
https://doi.org/10.4236/oalib.1113916

Received: July 5, 2025
Accepted: August 19, 2025
Published: August 22, 2025

Abstract

A complete open-loop, dual-axes Ku-band electromechanical system has been developed, implemented, and tested for the antenna positioning. The system is developed by using a magnetic positioning sensor AS5600, a PIC18F4553 controller, a microstepping driver STK672-080, and a hybrid stepper motor. A microstepping driver and magnetic positioning sensors are used to improve the system's performance. The system software is developed using MPLAB X v3.2 IDE. In the antenna mechanical assembly, the elevation over azimuth system is developed using worm gears with deep groove ball bearings. The satellite look angles are calculated using a GUI developed in C# for different satellites. The developed GUI and system are tested for angular displacement measurement and antenna positioning for Ku-band DTH service providers on geostationary satellites. The statistical measures mean, Standard Deviation, Relative Accuracy, Mean Absolute Error, and Root Mean Square Error are determined for the recorded angles for system performance. The developed electromechanical system shows a lower error profile.

Subject Areas

Applications of Communication Systems, Automata

Keywords

Antenna Measurements, Antenna Control System, Positioning Sensor, Angular Displacement Measurement

1. Introduction

The parabolic reflector antenna plays an important role in the satellite communication. As the beamwidth of the antenna is very small, the precise pointing is needed

at the transmitting and receiving ends [1] [2]. In general, the manual tracking and positioning techniques are used in antenna control. In this technique, the receiving antenna is rotated manually by operator in such a way that it receives maximum signal from the satellite. It is done by adjustment of the Earth station antenna look angles (combination of azimuth (A_Z) and (E_L) angles) and LNB skew. It is simple and easiest method of the antenna positioning. However, use of this method doesn't give the facility of an automatic tracking or positioning. Also, antenna alignment is labor or operator sensitive, time consuming, different for different types of satellites and locations of receivers [3]. The tracking or positioning parameters like error or speed depend on the experience of the operator in antenna control. The requirements of the antenna control are lower pointing error and antenna alignment within one tenth of its beamwidth [4].

If the user wants to access multiple satellites, they will have to set the antenna manually at different look angles for different satellites. The manual adjustments have limitations of antenna adjustments in the systems such as antenna parameter measurement systems [5] [6], antennas on mobile vehicles [7]-[16], antenna tracking systems or antenna positioning systems (APS), antenna systems working in natural disturbances [17]-[20], large and bulky antenna systems, etc. Also, the received signal quality (amplitude or strength) depends on the relative positions of the satellite and the antenna [21], and antenna parameters. After design of antenna, the antenna parameters become fixed. If the transmitted signal strength is fixed then the received signal quality depends on the antenna position in the form of its coordinates.

Therefore, an antenna positioning system is needed to align the antenna coordinates automatically to receive always the best quality and strongest satellite signal. With this consideration, it was proposed that an antenna positioning system be developed. In this paper, the design of subsystem for Ku-band satellite antenna positioning system is discussed.

The system is open loop type and implemented by selecting proper aspects for the antenna. The design aspects of electronic hardware and software for APS are positioning sensor AS5600, stepper motor, microstepping driver STK672-080, microcontroller PIC18F4553, compiler-XC8 with MPLAB X IDE and GUI development using C#.

The mechanical components for the system development under consideration are E_L over A_Z antenna mount, worm gear type and deep grove bearing. By integration and interfacing of mechanical hardware, electronic hardware and software, the final open loop APS is implemented for dual axes Ku band satellite antenna.

The performance analysis of the system implemented is presented in the last section.

2. Open Loop Aps

In the open loop system, the feedback path is absent, and the control unit receives control signals from positioning sensors. It is more applicable for a land to mo-

bile-satellite services. The shadowing and blocking effects are less significant in this system as the system uses positioning sensor outputs.

The positioning system for Ku-band parabolic antenna developed around the central control unit PIC18F4553 is presented in Figure 1. The E_L over A_Z mechanical arrangement is used in this system. Separate motor drives with microstepping (STK672-050), stepper motor, gear box (with worm gear) and positioning sensor (AS5600) are used for A_Z and E_L axes.

The keypad is used to enter the antenna positioning coordinates for a various satellites and the LCD displays current statues and parameters of the system. The true north is obtained by using digital compass and the horizontal by inclinometer. The positioning coordinates (A_Z and E_L) of the antenna are computed using the GUI. The computed coordinates are entered in the proper range using keypad, followed by "*" for next step. The system runs in two modes E_L positioning and A_Z positioning.

In the E_L positioning mode, the control unit reads the actual E_L angle from the positioning sensor coupled at A_Z axis. The output of the positioning sensor is in the voltage form and it depends on the actual absolute angle of the axis. This output is digitized by on-chip 12-bit ADC (of 18F4553), then computes the error between entered and actual E_L positioning angle. For a non-zero error, a stepper motor of the E_L axis rotates by one step. The process is repeated till the error becomes zero (with one bit hysteresis) and the actual positioning angle of the E_L is set. After the E_L positioning, the A_Z positioning mode is initiated. The process of the execution of the A_Z is similar to the E_L.

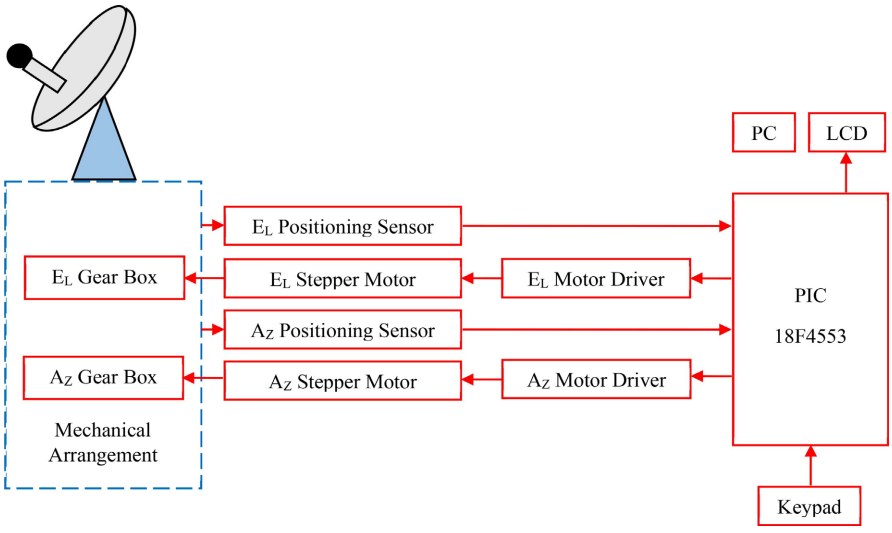

Figure 1. Elements of Ku-band open loop APS.

In A_Z positioning mode, the control unit reads the actual angle of the A_Z from the positioning sensor coupled to A_Z axis. Then it computes the error between entered and actual A_Z angle. For non-zero error, a stepper motor of the A_Z axis is rotated by one step. This process is repeated till the error becomes zero (with one

bit hysteresis) and the actual A_Z positioning angle is set. The final positioning of A_Z and E_L angles are displayed on the 16 × 2 LCD.

The A_Z and E_L axes are rotated by hybrid stepper motors arranged in unipolar mode. For accuracy, precision and resolution both A_Z and E_L motor drivers are designed with microstepping techniques [22]-[24]. The axes of the antennas are coupled to the motors using worm gears and ball groove bearings. The A_Z axis of the system can be rotated electronically between 0˚ - 359.9˚ and the E_L between 0˚ - 90.0˚.

3. Magnetic Position Sensors: AS56000

Two rotary magnetic Hall Effect potentiometers AS5600 are used in the proposed systems for the actual positioning angle measurement of A_Z and E_L axes. It is a 12-bit programmable contactless magnetic potentiometer whose output depends on the contactless rotary magnet position. It gives the output in the voltage form or on Inter Integrated Circuit (I^2C) bus. The advantages of AS5600 are its high reliability, durability, resolution, low power consumption, robust environmental tolerance and contactless angular displacement measurement [25]-[27]. For these sensors, measurable angular range from 0˚ to maximum (within 18˚ to 360˚) can be selected. The default range is 0˚ - 360˚. It measures the absolute angle from the north pole of the attached magnet with casing to axis [25] [26]. In the present development, for both axes, the default range (0˚ - 360˚) of the sensor is used. For further processing the analog voltage outputs of the sensors are connected to the analog channel of the microcontroller.

a) Resolution

For the default range, the output of the sensor is in between 0 to 5 V (for 0˚ = 0 V and 360˚ = 5 V). The on-chip signal conditioning is 12 bit. Thus, sensor resolution is,

$$\text{Resolution} = \frac{360^\circ}{2^{12}} \approx 0.088^\circ$$

b) Calibration of the Sensor

The actual satellite look angles are read from the positioning sensors with on chip ADC channels AN0 and AN1 of the PIC. The calibration is required to display actual and correct positioning angle on the LCD.

The positioning sensor is calibrated by using the Equations (1) - (4) for the angular displacement measurement.

$$X = 8 \times \text{adc\_out} \tag{1}$$

$$Y = \left(\left(\text{QUOTIENT}\left(X,7\right)\right) * 10\right) \tag{2}$$

$$Z = \text{QUOTIENT}\left(\left(\left(\text{MOD}\left(X,7\right)\right) * 14\right),10\right) \tag{3}$$

$$P = \text{QUOTIENT}\left(\left(Y + Z\right),13\right) \tag{4}$$

These equations are obtained by software and error reducing methods using the sensor resolution, on chip ADC resolution, ADC output (adc_out), protractor and

Microsoft excel. The same are implemented in the microcontroller software to measure the angular displacement.

The 12-bit ADC gives 0 output for the 0˚ and 4095 for 359.9˚. For 250.1˚, ADC gives $0B1D_{16} = 2845_{10}$, the Equation (1) gives 22,760, the Equation (2) gives 32,510, the Equation (3) gives 4, Equation (4) gives 2501, means displaying 250.1˚ on the LCD.

4. Control Unit (18F4553)

The selection of the components in control unit depends on the system requirements like speed, cost, on-chip resources, size, power consumption, etc. For the system consisting of positioning sensors and signal detectors, an onchip ADC PIC microcontroller is better option. The DSP and ARM will be the better options for high speed, high precision and modern algorithm systems. Microcontroller and DSP are useful for smoothing vibrations and mechanical resonances. Therefore, using these controllers the system performances are improved [22] [28]. The FPGA is useful for driving several motors simultaneously [29].

In the proposed system DIP 40 pin package PIC 18F4553 microcontroller is used because of easy and free development tools. It has better operating frequency, more onchip resources, technical support and application notes. It has onchip 12-bit ADC. Employed magnetic positioning sensors (AS5600) also have onchip 12-bit conditioning system. Thus, the use of 18F4553 will result in better system accuracy. Additional benefits of 18F4553 are 256 bytes EEPROM, 32 Kbytes flash program memory, C compiler optimized architecture, onchip USB bus, power management modes (run, idle and sleep), wide operating voltage range (2.0 V to 5.5 V) [30]. It is central control unit to control all the operations of the proposed positioning system. In the proposed system the 18F4553 pins are utilized for following assignments.

- RA0 (AN0): A_Z positioning sensor
- RA1 (AN1): E_L positioning sensor
- RE0 - RE2: A_Z axis motor driver control
- RA3 - RA5: E_L axis motor driver control
- RB0 - RB3: Keypad (Row lines)
- RB4 - RB7: Keypad (Column lines)
- RD4 - RD7: LCD data lines
- RD0, RD1, RD3: LCD control lines
- RC0: Control switch for mode selection
- RC6 (Tx): Serial data transmission
- RC7 (Rx): Serial data reception
- RD2: Testing LED and control bit (for selection of the mode),

The photograph of the 18F4553 microcontroller based system is presented in Figure 2.

5. User Interface

The user interface is required for interaction of user with developed APS. It is

needed for selection of various modes, entering positioning coordinates, sending commands to the system and displaying various parameters. In the proposed system a keypad and LCD are employed as user interface.

a) Keypad

The photograph of 4 × 4 matrix switch array keypad module is used to enter the look angles (A_Z and E_L) to access various satellites.

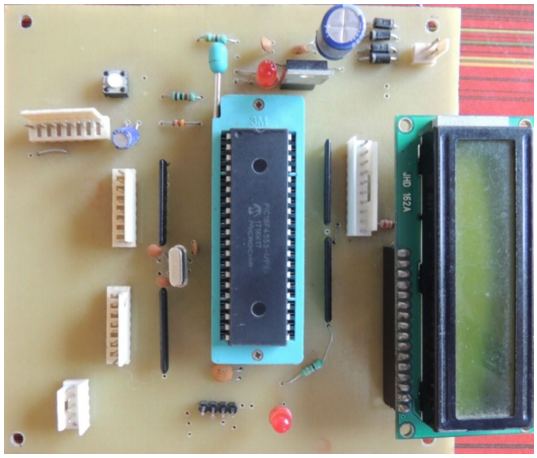

Figure 2. 18F4553 based system.

This type of the keypad module has total 16 buttons. All the buttons are alphanumeric digits with some special character. It has total eight terminals consisting of four rows and four columns. With polling method the PIC checks pressed key using a single port. A separate software module is developed for the keypad interfacing.

b) LCD

A 16 × 2 LCD is used to display the instructions, messages and parameters like entered positioning angle, positioning mode, step tracking mode, etc. and actual positioning angle of the system. It has three control lines (RW, RS, E), two supply lines (VDD, VSS), one contrast control line VEE and eight bit data lines (D0-D7). The control pins RS, RW and E are used to select the command or data registers, select read or write operation and enable LCD respectively. D7 pin has dual functions, data pin as well as busy flag (LCD statues pin).

The LCD is connected in the 4-bit mode. The D4 to D7 pins of the LCD are used and D0 to D3 are grounded. As it is connected in the 4-bit mode, it requires less number of microcontroller pins to send commands and data but this mode reduces speed of the microcontroller. The commands used during LCD initialization in 4-bit mode are listed in Table 1.

6. Motor Selection

The linear behavior of DC motors leads to the easy control and are used traditionally in tracking systems. The low life span and overheating of armature winding in DC motors limits the high-speed repetitive applications [1]. The high

Table 1. LCD commands for 4-bit mode.

Command	Function
28H	Use 2 lines, 5 × 7 matrix (4-bit mode)
01H	Clear screen
06H	Increment cursor
0EH	Cursor blinking, Display ON
80H	force cursor at the beginning of 1st line

torque characteristics for high efficiency, long operating life, high speed dynamic response, low noise and higher speed of PMBL DC motors are suitable but their higher cost and difficulties in repair limit their use in antenna control applications. The synchronous motors are fairly expensive and make the system complicated [5]. Due to the low power factor and less efficiency, induction motor is not suitable for antenna control applications. The maintenance of servomotor is expensive. The stepper motor is more effective in steering the antenna [31].

The characters of stepper motor viz. direct digital control, availability of torque at low speed and positioning without gears are helpful in the APS. Thus, in the proposed system, the stepper motor is preferred. A driver for motor depends on type of a motor used in the system.

Development of Microstepping Driver

The selection of proper driver mainly depends on the type, voltage and current rating of the motor. For stepper motor with stepping angle of 1.8˚ per step and gear ratio of 10:1, the positioning accuracy is 0.18˚ in full step mode and 0.09˚ in half step mode of the motor [5] [32]. Stepping error associated with stepper motors is reduced with the help of microstepping, high speed ratio of the gears and position sensors. The motor operations depend on the motor driver. For the present system, high torque unipolar stepper motors are used.

The important electrical and mechanical specifications of these motors are listed in **Table 2**.

Table 2. Specifications of stepper motor.

Parameter	Specifications
Stepping angle	1.8˚
Current per phase	1.2 A
Rated voltage	7.2 V
Holding torque	0.65 N-m
Resistance per phase	6 Ω
Stepping angle accuracy	±5%
Inductance per phase	4.3 mH
Operating voltage	18 - 37 V, DC

The complete circuit diagram of the motor driver is shown in Figure 3. It is developed by using optocoupler and microstepping driver.

a) Optocoupler, TLP521-4

It is used to isolate microcontroller system from high voltages of the microstepping driver and stepper motor. It improves the controller operation and reliability by eliminating interference [33].

In the present system, a TLP521-4 make optocouplers are used. Each optocoupler IC consists of a four LED-detector pair [34]. The recommended operating conditions are,

- Supply voltage, VCC = 5 V (typ.), 24 V (max.)
- LED forward current, IF = 16 mA (typ.), 25 mA (max.)
- Detector collector current IC = 1 mA (typ.), 10 mA (max.)

b) Microstepping Drives, STK672-080

In the present system, two STK672-080 microstepping drivers are used. These are sine wave drivers, with five modes of the operation and can reduce a step angle of the motor up to 1/16. These are MOSFET based hybrid IC types with driving capacity of 2.8 A load without heat sink. The important pins of STK672-080 are mentioned below.

- CLK: The input pulses are applied at this pin. The motor speed depends on CLK frequency. The input frequency range of pulses for this controller is 0 to 50 KHz with minimum pulse width of 10 μs [35].
- CCW: The direction of the stepper motor rotation depends on it. For CCW = 0, clockwise rotation, otherwise anticlockwise for CCW = 1.
- ENABLE: It is used to enable drive current of the motor.
- M3, M2 and M1: These pins are used to select proper microstepping mode out of five modes. In the present system, the 2W1-2 phase excitation mode is selected by setting M2 = 0, M1 = M0 = 1.
- MOI: It is a phase origin monitoring pin.
- V_{ref}: This pin is used to control the motor current.

For 1.2 A phase current (I_{OH}) motor,

$$V_{ref} = I_{OH} \times K \times R_s, \tag{5}$$

where,

K : Voltage divider ratio 4.7,

R_s : Internal current detector resistor = 0.15 Ω,

$\therefore V_{ref} = 1.2 \times 4.7 \times 0.15,$

$\therefore V_{ref} = 0.846$ V.

The phase current motor is adjusted by the use of preset connected at V_{ref} pin. For dual axes in the present system, two separate motor drivers are designed. Figure 4 presents the designed driver in the proposed system.

7. Power Supply

The microcontroller system is optically isolated from the stepper motor driving system. Hence, two separate power supplies are used. One is 5 V, 500 mA for mi-

crocontroller based system and another 24 V, 5 A for the stepper motor. The required +5 V for a driver circuit is derived from 24V, 5 A stepper motor supply.

8. Mechanical Arrangement

Two types of the mechanical arrangements are used in dual axes APS: E_L over A_Z and A_Z over E_L. The E_L over A_Z, where the E_L axis is coupled over the A_Z axis, is simple to design and easy for positioning. Hence, it is preferred in the present system. In this arrangement, the A_Z axis is rotated for complete circle, 0˚ to 360˚

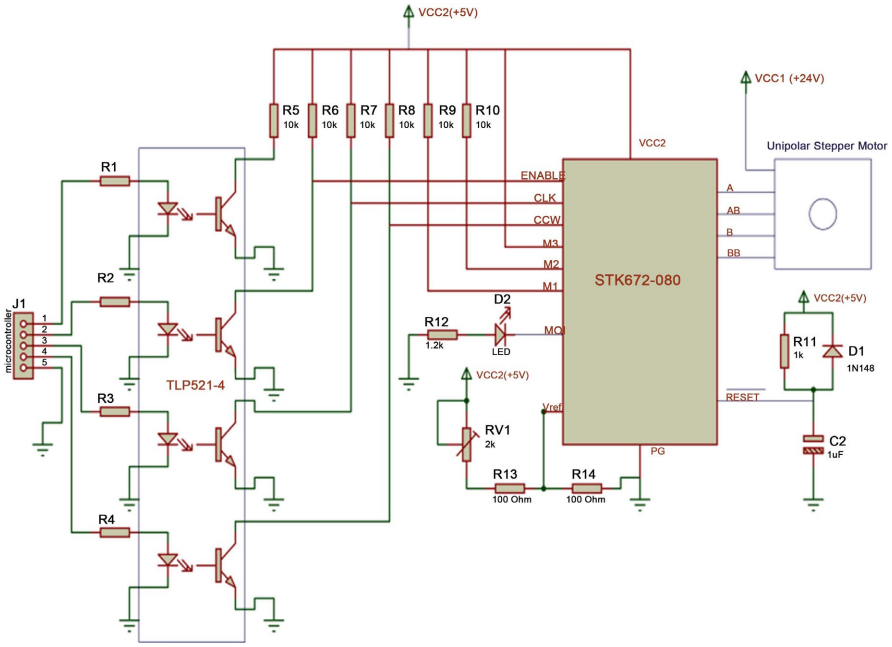

Figure 3. Microstepping driver for proposed APS.

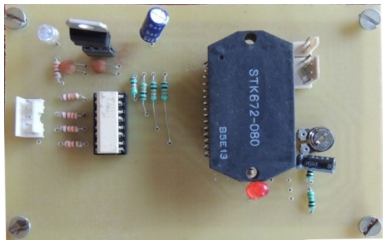

Figure 4. Designed microstepping driver.

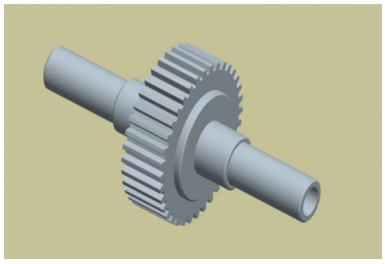

Figure 5. Gear CAD design.

Figure 6. Actual designed gear.

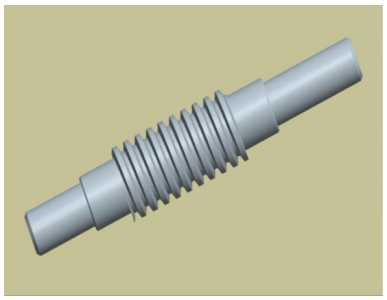

Figure 7. Worm CAD design.

Figure 8. Actual designed worm.

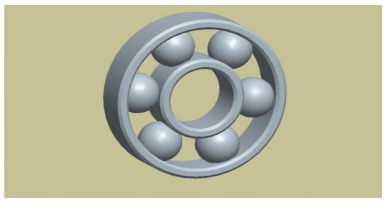

Figure 9. Bearing CAD design.

Figure 10. Actual designed bearing.

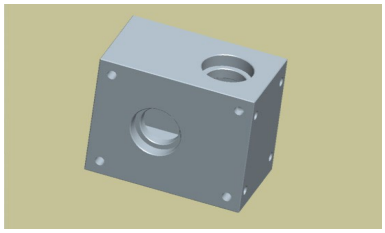

Figure 11. Gearbox CAD design.

Figure 12. Actual gearbox design.

Figure 13. Elements mechanical assembly.

Figure 14. Bearings of gear assembly.

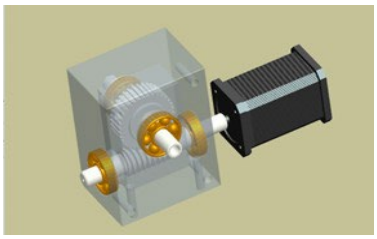

Figure 15. CAD design for gearbox assembly with motor.

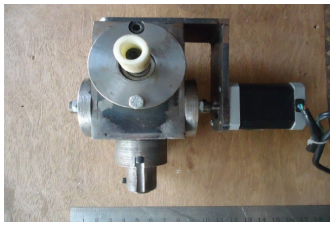

Figure 16. Actual designed gearbox assembly with motor.

Figure 17. EL assembly for antenna positioner.

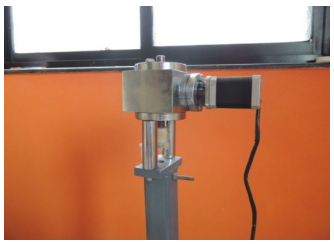

Figure 18. A_Z assembly for antenna positioner.

Figure 19. CAD design antenna positioner.

Figure 20. Photograph of actual design.

with respect to north and E_L axis between −40˚ to 230˚ with respect to horizontal plane. Figures 5-20 presents various elements and complete mechanical assembly of the present APS.

The gearbox in present system, consists of worm gear, bearings and shafts. The main part of the gearbox is worm gear. In the present system, single-threaded worm gears with 1:36 speed ratio are fabricated using EN19 steel material. The worm gear consists of a driver worm and driven worm. As the driver worm drives the driven worm, but the driven worm doesn't drive the driver worm, enabling locking, it is preferred in the system. The other advantages of worm gear in the antenna positioning are the high speed reduction ratio, increased torque, smooth gearing and high quality meshing ability [36]-[39].

For two axes, two separate gearboxes are designed. The friction and stress are reduced by installing two bearings of the deep groove ball type in each gearbox. The resolutions of gearbox in the present system are, 0.05˚ (without microstepping) and 0.007˚ (with microstepping of 1:8).

9. Dish Antenna

In the proposed system, an offset feed parabolic dish antenna is used. The specifications of the parabolic antenna in the present system are presented in Table 3.

Table 3. Specifications of parabolic antenna.

Parameter	Value
Gain @12.5 GHz	37 dBi
Survival wind	220 Km/h
Weight	2.25 Kg
Horizontal Axis	62 cm
Vertical Axis	68 cm

10. 18F4553 Software

The software designed with 18F4553 has following two parts.

a) Development of the libraries consisting of small program modules (subprograms) for each component of the system

b) Development of main program by accumulating all these modules (main program)

The MPLAB XC8 is supports 8-bit PIC families. This compiler runs with MPLAB version MPLAB X IDE v3.20 which is an open source platform, supporting more than 800 devices in code development and provides a single Integrated Development Environment for the microcontrollers. Therefore, the MPLAB XC8 is best suitable for proposed system development.

The system software is developed in XC8 using MPLAB X IDE. It consists of main program with several modules ledonoff(), lcd_init(), motor_init(), keypad_init(), angleazienter(), angleelventer(), adc1_init(), azimuth(), adc2_init(),

elevation(), azangleread() and elangleread() and the header files.

11. GUI for the System

The GUI provides interactive control to the user. In the present system the GUI is designed in the C# for calculation of satellite look angles. The screen shot of the GUI for the system is presented Figure 21.

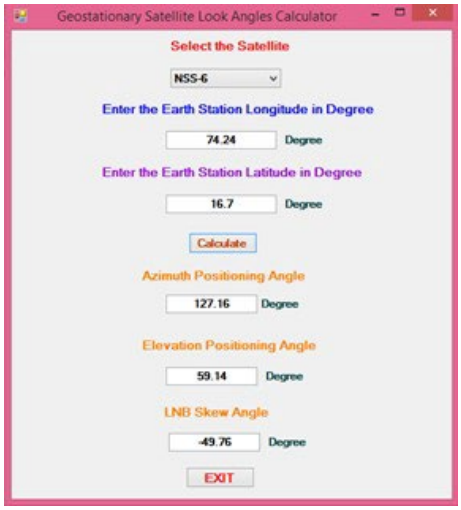

Figure 21. C# GUI for look angle calculation.

A visual studio is used for the development of the GUI. It provides a drag and drop facility to design GUI with C#. The use of C# is simple, easy to use and efficient for creation of the new GUI applications [39].

12. Geostationary Satellite Look Angles Calculator

The satellite look angles are the coordinates to which an Earth station antenna must be pointed to communicate with a satellite are called the look angles [40]. These angles are most commonly expressed as elevation (E_L) and azimuth (A_Z). To track or point directly a communication satellite, these angles are essential.

12.1. A_Z Angle

This angle is measured "eastward in clockwise sense from geographic north to the projection of the satellite path on local horizontal plane at the Earth station" [3]. Thus it is 0˚ and 180˚ at the North and South poles respectively.

The A_Z angle (θ) [4] [41] is given by,

$$\theta = 180 + \tan^{-1}\left(\frac{\tan d}{\sin L_{ae}}\right), \tag{6}$$

In another way

$$\theta = 180 + \frac{\sin d}{\sqrt{1-\cos^2 L_{ae}\cos^2 d}} \tag{7}$$

12.2. E_L Angle

This angle is measured vertically from the local horizontal plane at the Earth station to the satellite path. This angle is greater at the Earth station's equator and smaller at high latitudes.

The E_L angle (ϕ) [4] [41] is given by,

$$\phi = \tan^{-1}\left(\frac{\cos d \cos L_{ae} - (Re/r)}{\sqrt{1-\cos^2 d \cos^2 L_{ae}}}\right) \tag{8}$$

In another way,

$$\phi = \tan^{-1}\left(\cos\gamma - \frac{R_v}{r\sin\gamma}\right) \tag{9}$$

12.3. Polarization

The polarization of an electromagnetic wave means an orientation of the electric field in free space. The polarization might be linear or circular.

In the linear polarization, the local horizontal plane is skewed or tilted with the polarization of the satellite due to the following reasons,

a) the Earth curved surface.

b) different longitudes of the Earth station and the satellite.

This LNB skew (δ) is calculated using [42],

$$\delta = \tan^{-1}\left(\frac{\sin d}{\tan L_{ae}}\right) \tag{10}$$

Hence, to reduce the signal loss or attenuation the Earth station LNB skew adjustment must be required.

13. GUI Validation

The technique reported by Osman Emad Addeen Abdul Gabbar Mohammed [43] for validation of the GUI is used in the present system. The earth station longitude and the latitude are obtained by using GPS. The obtained coordinates are entered in the GUI during calculations. To test the developed GUI, the look angles for selected satellites are calculated for the known locations (Kolhapur, Longitude = 74.24˚ and Latitude = 16.70˚ and Karad, Longitude = 74.11˚ and Latitude = 17.18˚, India).

In the GUI, user can select a proper satellite, enter the required coordinates of earth stations (longitude and latitude) and calculate the look angles. The GUI developed is tested for geostationary satellites INSAT4A/GSAT10, ST-2, MEASAT-3, GSAT-15, NSS-6, ASIASAT-5 and SES-7. The GUI is upgradable for the various GEO and Non-GEO satellites. The look angles obtained in the GUI are validated using online "satsig" [44]. Both results, for two locations are compared in **Table 4** and **Table 5**.

From these tables it can be noticed that the look angles obtained in the GUI agree well with those from "satsig".

Table 4. GUI validation for Kolhapur, India (Longitude = 74.24˚ and Latitude = 16.70˚).

Satellite	A_Z (˚)		E_L (˚)		LNB Skew (˚)	
	"satsig"	GUI	"satsig"	GUI	"satsig"	GUI
83˚E INSAT-4A/GSAT-10	151.8	151.8	67.95	67.94	−26.91	−26.91
88˚E ST-2	139.56	139.56	64.80	64.79	−38.40	−38.40
91.5˚E MEASAT-3	132.77	132.77	62.11	62.10	−44.68	−44.68
93.5˚E GSAT-15	129.43	129.43	60.44	60.44	−47.71	−47.71
95˚E NSS-6	127.16	127.16	59.14	59.14	−49.76	−49.76
100.5˚E ASIASAT-5	120.22	120.22	54.12	54.11	−55.86	−55.86
108.2˚E SES-7	113.11	113.11	46.64	46.64	−61.76	−61.76

Table 5. GUI validation for Karad, India (Longitude = 74.11˚ and Latitude = 17.18˚).

Satellite	A_Z (˚)		E_L (˚)		LNB Skew (˚)	
	"satsig"	GUI	"satsig"	GUI	"satsig"	GUI
83˚E INSAT-4A/GSAT-10	152.10	152.10	67.38	67.38	−26.56	−26.56
88˚E ST-2	140.06	140.06	64.28	64.28	−37.83	−37.83
91.5˚E MEASAT-3	133.32	133.32	61.62	61.62	−44.03	−44.03
93.5˚E GSAT-15	130.00	130.00	59.98	59.97	−47.04	−47.04
95˚E NSS-6	127.74	127.74	58.69	58.69	−49.07	−49.07
100.5˚E ASIASAT-5	120.76	120.76	53.72	53.71	−53.18	−53.18
108.2˚E SES-7	113.58	113.58	46.30	46.30	−62.12	−62.12

In the developed system offset feed parabolic antenna is used. The offset feed arrangement has no aperture blocking. As the feed horn is directed upward, it is less sensitive to the noise from the ground [45]. The reflector shape of the received antenna system is elliptical, using major and minor axes, the offset angle is calculated.

$$\text{Offset angle} = \cos^{-1}\left(\frac{\text{Size of Minor axis}}{\text{Size of Major axis}}\right) \tag{11}$$

The offset must be considered during the final set of the E_L angle. The final E_L positioning angle is the offset angle calculated using Equation (11) and the inclination angle [43].

$$E_L \text{ angle} = \text{inclination} + \text{offset angle} - \phi \tag{12}$$

The disadvantages of the offset feed arrangement are the requirement of robust mechanical support and the difficulty of scanning [4].

The EL offset angle is 24.26˚ (calculated by using Equation (11)) and 24.2˚ ("satsig"). **Table 6** presents the E_L positioning angle for the offset feed calculated using Equation (12) and offset of 24.26˚.

14. Performance Analysis of the System

The performance of the developed system is analyzed by using the statistical measures. It is analyzed in two parts, system testing for the angular displacement measurement and APS validation.

Table 6. E_L angles for offset feed.

Satellite	E_L angles for offset feed (˚)
83˚E INSAT-4A/GSAT-10	46.3
88˚E ST-2	49.5
91.5˚E MEASAT-3	52.2
93.5˚E GSAT-15	53.8
95˚E NSS-6	55.1
100.5˚E ASIASAT-5	60.2
108.2˚E SES-7	67.6

14.1. Angular Displacement Measurement System

The developed system sensor module AS5600 and the calibrated output is validated for the angular displacement measurement by execution of ledonoff(), lcdinit(), adc1_init(), azimuth() and azangleread() modules.

It is tested for the angular displacement measurement for entered angle between 0 - 359 for the 60 readings selected by the random sampling method. The results displayed on the LCD are recorded. During testing, the angle is measured by bevel metallic protractor with actual setting values are recorded for A_Z and E_L modules. The system analysis for error and accuracy is done by using Equations (13) - (24) [46]-[49].

$$\bar{\theta} = \frac{1}{n}\sum_{i=1}^{n}\theta_i \tag{13}$$

$$\bar{\phi} = \frac{1}{n}\sum_{i=1}^{n}\phi_i \tag{14}$$

$$\sigma(\mathrm{A_Z}) = \sqrt{\frac{1}{n}\sum_{i=1}^{n}\left(\theta_i - \bar{\theta}\right)^2} \tag{15}$$

$$\sigma(\mathrm{E_L}) = \sqrt{\frac{1}{n}\sum_{i=1}^{n}\left(\phi_i - \bar{\phi}\right)^2} \tag{16}$$

$$\mathrm{MAE}(\mathrm{A_Z}) = \frac{1}{n}\sum_{i=1}^{n}\left|\theta_i - \theta'\right| \tag{17}$$

$$\mathrm{MAE}(\mathrm{E_L}) = \frac{1}{n}\sum_{i=1}^{n}\left|\phi_i - \phi'\right| \tag{18}$$

$$\mathrm{MAPE}(\mathrm{A_Z}) = \frac{1}{n}\sum_{i=1}^{n}\frac{\left|\theta_i - \theta'\right|}{\theta'}\times 100 \tag{19}$$

$$\mathrm{MAPE}(\mathrm{E_L}) = \frac{1}{n}\sum_{i=1}^{n}\frac{\left|\phi_i - \phi'\right|}{\phi'}\times 100 \tag{20}$$

$$A(A_Z) = 100 - MAPE(A_Z) \quad (21)$$

$$A(E_L) = 100 - MAPE(E_L) \quad (22)$$

$$RMSE(A_Z) = \sqrt{\frac{1}{n}\sum_{i=1}^{n}(\theta_i - \theta')^2} \quad (23)$$

$$RMSE(E_L) = \sqrt{\frac{1}{n}\sum_{i=1}^{n}(\phi_i - \phi')^2} \quad (24)$$

where,

θ_i = i^{th} actual value of the A_Z angle

θ' = entered A_Z angle for the selected satellite

$\overline{\theta}$ = mean of the actual value of A_Z angles

ϕ_i = i^{th} actual value of the E_L angle

ϕ' = entered E_L angle for the selected satellite

$\overline{\phi}$ = Mean of the actual value of E_L angles

n = number of repetitions

$\sigma(A_Z)$ = tandard Deviation at A_Z angles

$\sigma(E_L)$ = Standard Deviation at E_L angles

$MAPE(A_Z)$ = Mean Absolute Percentage Error for A_Z angles

$MAPE(E_L)$ = Mean Absolute Percentage Error for E_L angles

$A(A_Z)$ = Positioning Sensor Relative Accuracy for A_Z angles

$A(E_L)$ = Positioning Sensor Relative Accuracy E_L Angle

$RMSE(A_Z)$ = Root Mean Square Error of the A_Z angles

$RMSE(E_L)$ = Root Mean Square Error of the E_L angles

The error and accuracy parameters analyzed are presented in Table 7.

Table 7. Performance parameters for angular displacement.

Parameter	A_Z	E_L
Mean absolute error (MAE)	0.208˚	0.223˚
Standard deviation (SD) of error	0.224˚	0.219˚
Mean absolute percentage error (MAPE)	0.339%	0.347%
Relative accuracy (A)	99.66%	99.62%

Table 8. Statistical analysis (Mean and SD) of developed APS.

Satellite	Satellite look angles from GUI A_Z˚/E_L˚	Mean A_Z˚/E_L˚	SD A_Z˚/E_L˚
83 ˚E INSAT-4A/GSAT-10	151.8/46.3	151.75/46.32	0.26/0.23
88˚E ST-2	139.6/49.5	139.76/49.43	0.24/0.27
91.5˚E MEASAT-3	132.8/52.2	132.78/52.09	0.24/0.23
93.5˚E GSAT-15	129.4/53.8	129.50/53.76	0.28/0.27
95˚E NSS-6	127.2/55.1	127.24/55.20	0.27/0.25
100.5˚E ASIASAT-5	120.2/60.2	120.26/59.27	0.22/0.21
108.2˚E SES-7	113.1/67.6	113.08/67.6	0.24/0.24

Table 9. Statistical analysis (MAE and RMSE) of developed APS.

Satellite	Positioning angles A_Z°/E_L°	MAE A_Z°/E_L°	RMSE A_Z°/E_L°
83 ˚E INSAT-4A/GSAT-10	151.8/46.3	0.22/0.20	0.25/0.22
88˚E ST-2	139.6/49.5	0.21/0.19	0.24/0.23
91.5˚E MEASAT-3	132.8/52.2	0.20/0.24	0.23/0.25
93.5˚E GSAT-15	129.4/53.8	0.25/0.24	0.28/0.27
95˚E NSS-6	127.2/55.1	0.23/0.24	0.26/0.26
100.5˚E ASIASAT-5	120.2/60.2	0.20/0.25	0.23/0.28
108.2˚E SES-7	113.1/67.6	0.21/0.20	0.23/0.24

From Table 7, it can be noted that the relative accuracy attained for positioning sensors in A_Z and E_L in the present system is more than 99%. The angular measurement system has lower error profile.

14.2. APS

In India, INSAT-4A/GSAT-10, ST-2, MEASAT-3, GSAT-15, NSS-6, Asiasat-5 and SES-7 satellites are providing DTH services. Thus, in the system under investigation, the longitude data of these satellites are used to position the earth station receiving antenna. The look angles for the satellites obtained from GUI are entered using the keypad. The final position angles computed by the system are displayed on LCD. The process is repeated 20 times for each satellite at 28°C. Thus, using GUI and LCD data, the system under investigation is analyzed with statistical measures using Equations (13) - (24). The performance in the form of mean, SD, MAE and RMSE for the recorded angles are presented in Table 8 and Table 9.

The Mean Absolute Error and Root Mean Square Error represent the error profile of the developed system. The average Mean Absolute error for A_Z and E_L in the developed system is 0.217˚ and 0.220˚, respectively. The average is for seven different satellites. The Root Mean Square Error for A_Z and E_L is 0.245˚ and 0.250˚, respectively. The smaller value of these parameters indicates a lower error profile and higher accuracy.

Also, the average Standard Deviation for A_Z and E_L is 0.250˚ and 0.242˚, respectively. It gives the precision of the systems, lowers its value, higher the system precision.

15. Conclusions

The complete system positioning error depends on the mechanical assembly and positioning sensors; hence received signal quality is independent on the actual signal quality, and thus the system has no shadowing and blocking effects.

The system is designed by selecting appropriate aspects such as an antenna, magnetic positioning sensors, control unit, motor, motor driver and gears. The result of that gives better system performance and reduces the system cost.

The worm gear provides the locking facility; it locks the antenna at stationary and minimizes the environmental disturbance's effect. Increasing the gear ratio reduces the torque and the required motor power.

The system motor drivers are designed with microstepping, providing a low-cost solution to improve system accuracy. The system control unit is developed using readily available PIC 18F4553. Its cost is less than other same features processors.

Conflicts of Interest

The authors declare no conflicts of interest.

References

[1] Bolandhemmat, H., Fakharzadeh, M., Mousavi, P., Jamali, S.H., Rafi, G.Z. and Safavi-Naeini, S. (2009) Active Stabilization of Vehicle-Mounted Phased-Array Antennas. *IEEE Transactions on Vehicular Technology*, **58**, 2638-2650. https://doi.org/10.1109/tvt.2008.2012159

[2] Lo, V.Y. (1996) Ka Band Monopulse Antenna-Pointing Systems Analysis and Simulation. TDA Progress Report (42-124), 104-112.

[3] Cesar, R.M., *et al.* (2012) Development of an Automated System for Maneuvering Parabolic Dish Antennas Used in Satellite Communication. *ABCM Symposium Series in Mechatronics—Section-II, Control System*, **5**, 69-78.

[4] Dennis, R. (2006) Satellite Communications. McGraw-Hill Education.

[5] Papaioannou, D. and Langley, R.J. (1983) A Microcomputer Based Control System for Antenna Measurements. *Journal of Physics E: Scientific Instruments*, **16**, 394-396. https://doi.org/10.1088/0022-3735/16/5/008

[6] Bekasiewicz, A., Koziel, S. and Czyz, M. (2023) Time-Gating Method with Automatic Calibration for Accurate Measurements of Electrically Small Antenna Radiation Patterns in Non-Anechoic Environments. *Measurement*, **208**, Article ID: 112477. https://doi.org/10.1016/j.measurement.2023.112477

[7] Kim, M., Kim, J. and Yang, O. (2013) Precise Attitude Control System Design for the Tracking of Parabolic Satellite Antenna. *International Journal of Smart Home*, **7**, 275-290. https://doi.org/10.14257/ijsh.2013.7.5.27

[8] Tseng, H.C. and Teo, D.W. (1995) Ship-Mounted Satellite Tracking Antenna with Fuzzy Logic Control. *Proceedings of International Conference on Control Applications*, Albany, 28-29 September 1995, 549-553. https://doi.org/10.1109/cca.1995.555785

[9] Watanabe, T., Ogawa, M., Nishikawa, K., Harada, T., Teramoto, E. and Morita, M. (1996) Mobile Antenna System for Direct Broadcasting Satellite. *IEEE Antennas and Propagation Society International Symposium*. 1996 *Digest*, Baltimore, 21-26 July 1996, 70-73. https://doi.org/10.1109/aps.1996.549544

[10] Ming, A., Yamaoka, T., Kida, T., Kanamori, C. and Satoh, M. (2005) Accuracy Improvement of Ship Mounted Tracking Antenna for Satellite Communications. *IEEE International Conference Mechatronics and Automation*, 2005, Niagara Falls, 29 July-1 August 2005, 1369-1374. https://doi.org/10.1109/icma.2005.1626753

[11] Kim, J., Park, S. and Jin, T. (2006) Simplified Fuzzy-Pid Controller of Data Link Antenna System for Moving Vehicles. In: Yang, Q. and Webb, G., Eds., *PRICAI* 2006:

Trends in Artificial Intelligence. *PRICAI* 2006, Springer, 1083-1088. https://doi.org/10.1007/978-3-540-36668-3_138

[12] Edgar, A., *et al.* (2007) Control System for the Antenna Positioning. *Proceeding of the 7th WSEAS International Conference on Applied Informatics and Communication*, Athens, 24-26 August 2007, 390-392.

[13] Chang, P. and Lin, J. (2008) Mobile Satellite Antenna Tracking System Design with Intelligent Controller. *WSEAS transactions on System and Control*, **3**, 435-446.

[14] Wen, C., Lu, J. and Su, W. (2021) Bi-Objective Control Design for Vehicle-Mounted Mobile Antenna Servo Systems. *IET Control Theory & Applications*, **16**, 256-272. https://doi.org/10.1049/cth2.12203

[15] Soltani, M.N., Izadi-Zamanabadi, R. and Wisniewski, R. (2011) Reliable Control of Ship-Mounted Satellite Tracking Antenna. *IEEE Transactions on Control Systems Technology*, **19**, 221-228. https://doi.org/10.1109/tcst.2010.2040281

[16] Basari, Saito, K., Takahashi, M. and Ito, K. (2010) Field Measurement on Simple Vehicle-Mounted Antenna System Using a Geostationary Satellite. *IEEE Transactions on Vehicular Technology*, **59**, 4248-4255. https://doi.org/10.1109/tvt.2010.2066997

[17] Cho, C., Lee, S.H., Kwon, T.Y. and Lee, C. (2003) Antenna Control System Using Step Tracking Algorithm with H_∞ Controller. *International Journal of Control, Automation, and Systems*, **1**, 83-91.

[18] Yalcin, Y. and Kurtulan, S. (2009) A Rooftop Antenna Tracking System: Design, Simulation, and Implementation. *IEEE Antennas and Propagation Magazine*, **51**, 214-224. https://doi.org/10.1109/map.2009.5162072

[19] Hao, L. and Yao, M. (2011) SPSA-Based Step Tracking Algorithm for Mobile DBS Reception. *Simulation Modelling Practice and Theory*, **19**, 837-846. https://doi.org/10.1016/j.simpat.2010.11.009

[20] Hoque, M.A. and Hassan, A.K. (2015) Modeling and Performance Optimization of Automated Antenna Alignment for Telecommunication Transceivers. *Engineering Science and Technology, an International Journal*, **18**, 351-360. https://doi.org/10.1016/j.jestch.2015.01.002

[21] Gawronski, W. (2002) Control and Pointing Challenges of the NASA Deep Space Network Antennas. *8th IEEE International Conference on Methods and Models in Automation and Robotics*, Szczecin, 2-5 September 2002.

[22] Bellini, A., Concari, C., Franceschini, G. and Toscani, A. (2007) Mixed-Mode PWM for High-Performance Stepping Motors. *IEEE Transactions on Industrial Electronics*, **54**, 3167-3177. https://doi.org/10.1109/tie.2007.905929

[23] Yuen, L.C. and Ehkan, P. (2018) Design and Implementation of FPGA Based Bipolar Stepper Motor Controller for Linear Slide Application. *Journal of Telecommunication, Electronic and Computer Engineering* (*JTEC*), **10**, 85-88.

[24] Song, Y.L. and Bai, C.X. (2012) Research and Analysis of Image Processing Technologies Based on Dotnet Framework. *Physics Procedia*, **25**, 2131-2137. https://doi.org/10.1016/j.phpro.2012.03.360

[25] Essaadaoui, R., El Hadi, M., Ouariach, A., Moussaouy, A.E., Hachmi, A. and Mommadi, O. (2021) Construction of an Innovative, Modern and Affordable Teaching Tool in Practical Classroom Activities Using AS5600 Encoder. *Physics Education*, **56**, Article ID: 063006. https://doi.org/10.1088/1361-6552/ac27f5

[26] Zeng, D., Wang, Z., Wang, M., Eichstaedt, O. and Yuan, H. (2017) Automatic Bio-Sampling System Based on Micro-Injection Pump and Pneuamtic Micro Valves. 2017 *Chinese Automation Congress* (*CAC*), Jinan, 20-22 October 2017, 4140-4146.

https://doi.org/10.1109/cac.2017.8243506

[27] Sanz, J.M., Reyes, V., Sanz, A. and Guerreira, J. (2019) A New PLC Stack for Distributed and Synchronous Configurations. 2019 1*st Global Power, Energy and Communication Conference* (*GPECOM*), Nevsehir, 12-15 June 2019, 50-55. https://doi.org/10.1109/gpecom.2019.8778456

[28] Bendjedia, M., Ait-Amirat, Y., Walther, B. and Berthon, A. (2012) Position Control of a Sensorless Stepper Motor. *IEEE Transactions on Power Electronics*, **27**, 578-587. https://doi.org/10.1109/tpel.2011.2161774

[29] Carrica, D., Funes, M.A. and Gonzalez, S.A. (2003) Novel Stepper Motor Controller Based on FPGA Hardware Implementation. *IEEE/ASME Transactions on Mechatronics*, **8**, 120-124. https://doi.org/10.1109/tmech.2003.809160

[30] Microchip Technology. https://www.microchip.com

[31] Holleboom, K. (1987) Self-Learning Step Track System to Point an Antenna at a Geostationary Satellite Using a PC. *IEEE Transactions on Consumer Electronics*, **33**, 481-487. https://doi.org/10.1109/tce.1987.290224

[32] Min, K., *et al.* (2000) A Basic Study on the Azimuth Tracking Algorithm for Mobile DBS Reception Antenna System. *Proceedings of ISAP* 2000, Fukuoka, 21-25 August 2000.

[33] Cheng, Y.Z., Chen, Y. and Wang, H.X. (2011) Design of PID Controller Based on Information Collecting Robot in Agricultural Fields. 2011 *International Conference on Computer Science and Service System* (*CSSS*), Nanjing, 27-29 June 2011, 345-348. https://doi.org/10.1109/csss.2011.5974664

[34] https://www.mouser.in/pdfdocs/AMS_AS5600_Datasheet_EN.PDF

[35] https://docs.rs-online.com/9065/0900766b811a65f9.pdf

[36] He, Y., Li, G.F., Zhao, Y.P., Sun, Y. and Jiang, G.Z. (2018) Numerical Simulation-Based Optimization of Contact Stress Distribution and Lubrication Conditions in the Straight Worm Drive. *Strength of Materials*, **50**, 157-165. https://doi.org/10.1007/s11223-018-9955-z

[37] Dobreva, A., Dobrev, V. and Mollova, G. (2022) Research of Gear Drives. *IOP Conference Series*: *Materials Science and Engineering*, **1220**, Article ID: 012025. https://doi.org/10.1088/1757-899x/1220/1/012025

[38] Pavlenko, S. and Mascenik, J. (2021) Dynamic Load of Teeth of Cylindrical Worm Gear. In: Knapčíková, L., Peraković, D., Behúnová, A. and Periša, M., Eds., *EAI/Springer Innovations in Communication and Computing*, Springer, 351-361. https://doi.org/10.1007/978-3-030-67241-6_28

[39] Pavlenko, S., Mascenik, J. and Krenicky, T. (2022) Mathematical Modeling of Drive and Dynamic Load of Teeth of Cylindrical Worm Gear. In: Knapčíková, L., Peraković, D., Behúnová, A. and Periša, M., Eds., *EAI/Springer Innovations in Communication and Computing*, Springer, 61-83. https://doi.org/10.1007/978-3-030-90462-3_5

[40] Pratt, T. and Allnutt, J.E. (2019) Satellite Communications. John Wiley & Sons.

[41] Kolawole, M.O. (2017) Satellite Communication Engineering. CRC Press.

[42] Telecommunications Satellite Communications: Satellite Orbits, Coverage, and Antenna Alignment. https://labvolt.festo.com/downloads/87768_f0.pdf

[43] Alhasan, E.A.G.M. (2018) A Design of Automatic Dish-Antenna Positioning System for Receiving Geo-Satellites Signals. Ph.D. Thesis, University of Gezira.

[44] Satellite Signal. https://www.satsig.net/ssazelm.htm

[45] Kraus, J.D., Marhefka, R.J. and Khan, A.S. (2011) Antennas and Wave Propagation. McGraw Hill.

[46] Kalsi, H.S. (2010) Electronic Instrumentation. 3rd Edition, Tata McGraw-Hill Education.

[47] Bandong, S. and Joelianto, E. (2019) Counting of Aedes Aegypti Eggs Using Image Processing with Grid Search Parameter Optimization. 2019 *International Conference on Sustainable Engineering and Creative Computing* (*ICSECC*), Bandung, 20-22 August 2019, 293-298. https://doi.org/10.1109/icsecc.2019.8907232

[48] Khair, U., Fahmi, H., Hakim, S.A. and Rahim, R. (2017) Forecasting Error Calculation with Mean Absolute Deviation and Mean Absolute Percentage Error. *Journal of Physics*: *Conference Series*, **930**, Article ID: 012002. https://doi.org/10.1088/1742-6596/930/1/012002

[49] Dimitriadou, S. and Nikolakopoulos, K.G. (2022) Development of the Statistical Errors Raster Toolbox with Six Automated Models for Raster Analysis in GIS Environments. *Remote Sensing*, **14**, Article 5446. https://doi.org/10.3390/rs14215446